Classification of Spine Abnormalities using Deep Learning

Muhammad Shahrul Zaim bin Ahmad
Faculty of Engineering & Technology, Multimedia University

Nor Azlina Ab. Aziz
Faculty of Engineering & Technology, Multimedia University

Lim Heng Siong
Faculty of Engineering & Technology, Multimedia University

https://doi.org/10.5109/7323381

出版情報：Proceedings of International Exchange and Innovation Conference on Engineering & Sciences (IEICES). 10, pp.998-1004, 2024-10-17. International Exchange and Innovation Conference on Engineering & Sciences
バージョン：

Classification of Spine Abnormalities using Deep Learning

Muhammad Shahrul Zaim bin Ahmad, Nor Azlina Ab. Aziz*, Lim Heng Siong
Faculty of Engineering & Technology, Multimedia University, 75450 Melaka, Malaysia
*azlina.aziz@mmu.edu.my

Abstract: *The spine provides structural support for the body. Identifying spinal abnormalities is crucial for assessing spinal health. Deep learning has gained popularity due to better performance compared to the traditional machine learning approaches. This study investigates the performance of a deep learning model in classifying different types of spinal abnormalities, namely scoliosis, spondylosis, and lesions using x-ray images. The deep learning model is trained and evaluated using two public datasets. The images in the first dataset are labelled to three classes; scoliosis, spondylosis, and normal, while the images in the second dataset are labelled to normal and lesion. The model was trained and tested on four different classification tasks. The deep learning model achieved accuracy of 100% for two binary and one multiclass classification of images from the first dataset and 97.5% accuracy for binary classification of images from the second dataset. The classification model would be a beneficial tool for medical professionals to perform initial diagnosis.*

Keywords: Deep learning; spine abnormalities; scoliosis, spondylosis, lesion.

1. INTRODUCTION

Artificial intelligence (AI) has been extremely popular among the research community for the last decade. The involvement of AI has brought a lot of advantages to various fields. AI can be implemented for various use cases such as in autonomous vehicles [1], automatic checkout system for grocery shopping [2], home security [3], facial recognition for class attendance [4], smart agriculture [5], defect detection in manufacturing [6], disaster prevention [7], and medical image analysis [8]. For medical images, AI has been adopted for cancer detection in different parts of the body such as lung [9], bladder [10], breast [11], and prostate [12]. Additionally, AI is also utilized to analyze brain condition [13–17]. The usage of AI can also be seen in musculoskeletal analysis such as bone fracture detection [18] and knee joint segmentation [19].

AI approaches can be categorized as traditional machine learning and deep learning. The performance of the deep learning model is observed to provide better accuracy and sensitivity compared to traditional machine learning methods such as logistic regression, support vector machines, decision trees, and Bayesian Point Networks [20].

The spine provides structural support for the body, especially the head and trunk. Maintaining spinal health is vital to overall health and well-being. Multiple deep learning methods are available to perform analysis on the spine, including, segmentation of the spine [21], object detection [22], landmark localization [23], and classification [24].

Classification can be used in performing diagnosis on multiple spinal pathologies. Classification can be done for monitoring and diagnosing patients with scoliosis. The deep learning can be used to predict scoliosis shape [24], and scoliosis progression [25]. Classification can also be applied to identify lumbar degenerative diseases [26], vertebral compression fracture [27–29], foraminal stenosis [30], and osteoporosis [31].

In this study, a deep learning-based classification model is developed to differentiate x-ray images of normal spines and spines with abnormalities. This study aims to investigate the performance of deep learning models on different classification tasks. The classification tasks include binary classification and multiclass classification on two publicly available datasets which are the Thailand's Burapha University (BUU) dataset and the x-ray vertebrae dataset from King Abdullah University Hospital, Jordan University of Science and Technology, Jordan. The classes of the x-ray vertebrae dataset can be divided into normal, spondylolisthesis, and scoliosis. The BUU dataset consists of normal spines and spines with lesions. The results show that the proposed deep learning model can achieve very high accuracy results ranging from 97.5-100%.

This paper is organized by dividing it into five chapters. The first and current chapter is the introduction which includes the background of the study. The second chapter is the materials, which include the dataset implemented in this study. The third chapter is the methodology, where the pipeline, architecture, and training process of the model utilized in this study are explained further. The fourth chapter is the result and discussion. Chapter four discusses the results obtained using the methodology proposed in chapter three. Finally, the last chapter, chapter five, concludes the findings of this study.

2. MATERIALS

2.1 X-ray vertebrae dataset

The first dataset used in the classification model is vertebrae x-ray images that have been labelled as normal, spondylolisthesis, and scoliosis. The dataset includes 338 subjects where 240 of them are females and 98 are males. The dataset is available from Kaggle (https://www.kaggle.com/datasets/yasserhessein/the-vertebrae-xray-images). Further information on the dataset is included in Table 1.

The images in this dataset consist of different resolutions. The resolutions available in the datasets are the original size, and a few square-shaped images ranged from 224 pixels to 331 pixels for each side. The images have been classified into folders which are normal, *scol* (scoliosis), and *spond* (spondylolisthesis). In Fig. 1, images from the dataset are displayed. Starting from the left is the normal, scoliosis, and spondylolisthesis spine.

Table 1. Vertebrae x-ray dataset information

	Total	Female	Male
Normal	71	40	31
Scoliosis	188	151	37
Spondylolisthesis	79	49	30

Fig. 1. Example of images from vertebrae x-ray dataset from Kaggle

2.2 BUU Spine Dataset

The second dataset is the BUU Spine Dataset [32]. The datasets include 400 subjects. Each subject has a pair of X-ray images, each from an anterior-posterior (AP) and lateral view. The dataset includes different resolutions of images. The images were labelled with the coordinate of the lumbar vertebral corners (L1-L5). Additionally, the dataset also includes lesion labelling at the specific lumbar spine segments. The vertebrae corner and lesion labelling are included in the CSV files for all images. The subjects included in the dataset are 127 male and 273 female. The ages ranged from 6 to 89 years old.

Furthermore, each X-ray image and subsequent CSV file was named according to a specific format. The first four digits are the ID of the image, followed by the sex of the subject, M for male and F for female. The next three digits are the age of the subject, followed by a Y representing "year old". The last digit is either 0 or 1 where 0 is to label the image for AP view and 1 for lateral view. For example, if the image is labelled as "0012-F-013Y1" means that the ID of the image is "0012", the gender of the subject is female, she is 13 years old, and the image is in lateral view.

In this study, only the lateral images are used for the classification task. The reason is that most of the lesion types diagnosed in the dataset are only visible in the lateral view. Fig. 2 shows the AP and lateral x-ray of normal spine, while Fig. 3 shows the AP and lateral x-ray of patient with lesion in the spine.

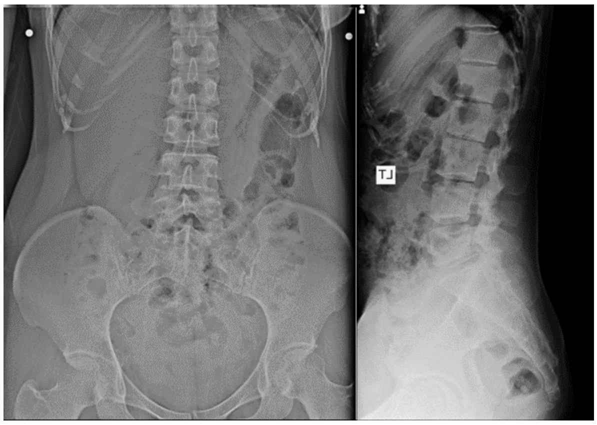

Fig. 2. A pair of images from a normal patient in the BUU spine dataset

Fig. 3. A pair of images from a patient with a lesion in the BUU spine dataset

3. METHODOLOGY

3.1 Data Preprocessing

The data preprocessing methods alter or improve the original datasets to fit the requirement of the deep learning model. The file types required by the input of the deep learning model are JPG, JPEG, BMP, and PNG. To ensure that the program can run properly with new data, non-image file or image file with different file types are removed from the dataset. The images are then resized from their original image size to a specific input resolution which is 224×224×3.

Then, the images are grouped into batches, where the batch sizes are changed according to the dataset size for each classification task to ensure proper distribution in the training, validation, and testing set. Batch size is the amount of data used as input before the weights in the model are updated. The batch size is set between 20 and 26. The data in the batch contain the pixel information and the label for each image. Furthermore, the pixel value was also normalized from the original value of 0 to 255, ensuring the pixels have a range of [0 to 1], by dividing the pixel value by 255.

The datasets are then divided into three sets which are training, validation, and testing set. The training set is used to train the model and update the weights. The validation set is used to tune the model's hyperparameters. The process is done by changing the parameters and choosing the model that performs best on the validation dataset [33]. The test set is an external set used to evaluate the overall performance of the deep model after it has been trained on the training and validation set. In the classification model, the ratio of the images used for training, validation, and test set are 60%, 20%, and 20%. However, due to the limited amount of data and a small number of batches available after division, the ratio is not exact.

3.2 Model Architecture

The proposed model used is sequential, a type of model available in Keras and TensorFlow. The sequential model is a simple model where the neural networks include a single stack of layers, and the layers are connected sequentially [33]. The model consisted of 8 layers including maxpooling and dense layers. The number of convolutional layers is 3. The model architecture is displayed in Fig. 4.

The first, third, and fifth layers consist of the convolutional layer. The convolutional network in the first and fifth layers consists of 16 filters, a kernel size of 3×3, and a stride of one. The kernel size and stride were constant through the convolutional layers. The third layer consists of 32 filters. The activation function used is Rectified Linear Unit (ReLU) where the negative values from the input of the neurons are set to zero.

After each convolutional layer, a pooling layer is added. A pooling layer is added to reduce the size of the feature maps (width and height), where smaller feature maps have lower computational complexity. The pooling operation of choice is Max Pooling where the maximum value within a pixel size of 2×2 is used. This means that the width and height of the feature maps were reduced by half for each of them. After the convolutional layers and pooling layers, a flatten layer is added to change the 2D feature maps from the convolutional and pooling layers into a 1D vector. This is done because dense layers require a 1D vector as an input.

The last two layers are dense layers. The dense layers are used to make predictions according to the feature maps that have been flattened into 1D vectors. The first dense layer consists of 256 neurons while the second layer neurons depend on the number of classes to be predicted. In this work, the number of classes is either two or three. For two classes, binary classification is done where the last dense layer only consists of one neuron, and the neuron value ranges between zero and one. The prediction is done by representing a class as zero and the other as 1. The activation function used is sigmoid for binary classification. For multiclass classification (class: n>2), the number of neurons is similar to the number of classes. For three class classifications, three neurons are used.

The activation function used varies depending on the number of classes included during the classification process. For binary classification, the activation function employed is the sigmoid function. The sigmoid function is defined as shown in equation (1).

$$\sigma(x) = \frac{1}{1 + e^{-x}} \qquad (1)$$

The sigmoid function outputs a value that ranges between 0 and 1. Sigmoid is used for a binary classification task where the output can represent the probability for two classes. If the sigmoid function is closer to zero ($\sigma(x)$<0.5), the function predicts the first class while if the output is closer to 1 ($\sigma(x)$>0.5), the function is predicting the second class.

For multiclass classification, the softmax function is utilized. Softmax provides probability distribution over multiple classes. The function for determining the probability of each class is defined as below:

$$\sigma(z)_i = \frac{e^{z_i}}{\sum_{j=1}^{K} e^{z_j}} \qquad (2)$$

Where the input of the softmax function is a vector z that contains K real numbers. The sum of output for all the classes is one and the range of value for each class is between 0 and 1. A higher value indicates a higher probability of the class present in the image.

3.3 Training

For training the deep learning model, the optimizer used is Adaptive Moment Estimation also called Adam [34]. Adam is an adaptive learning rate algorithm where the learning rate is adjusted dynamically, making tuning the learning rate hyperparameter less necessary. The loss function chosen for training the binary classification is binary cross entropy. The function evaluates the model's ability to predict the labels correctly and is used for binary classification problems.

The number of epochs in the model trained is 20. One epoch consists of a cycle in which the entire training and validation dataset is used to train the deep-learning model. For each epoch, the deep learning model was updated over several iterations, where the number of iterations is the size of the training dataset divided by the batch size.

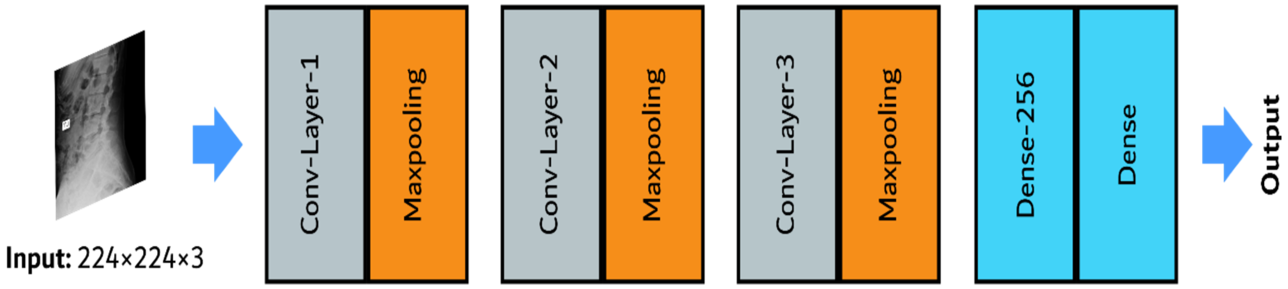

Fig.4 SEQ Fig._ * ARABIC 4. Architecture of the deep learning model evaluated in this study.

4. RESULT AND DISCUSSION

4.1 Vertebrae X-ray Images

Three classes of spine are available in the vertebrae x-ray dataset which are normal, scoliosis, and spondylolisthesis. The result will be evaluated through two different tasks which are binary classification – a combination of scoliosis or spondylolisthesis with normal and three-class classification.

4.1.1 Scoliosis and Normal Spine

The first task the deep learning model tested is a binary classification of scoliosis and normal spine. Fig. 5 displays the labeling of the spine images as either normal or scoliosis. Normal spine images are labeled 0 and spines with scoliosis are labeled 1. The images are then used as input for the deep learning model. Fig. 6 displays the graph of training accuracy vs. validation accuracy in 20 epochs. It is observed that the testing accuracy of the deep learning model increased to more than 95% after 15 epochs.

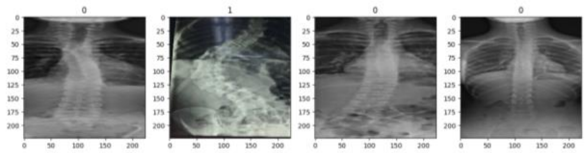

Fig. 5. Labeling of images in scoliosis versus normal classification

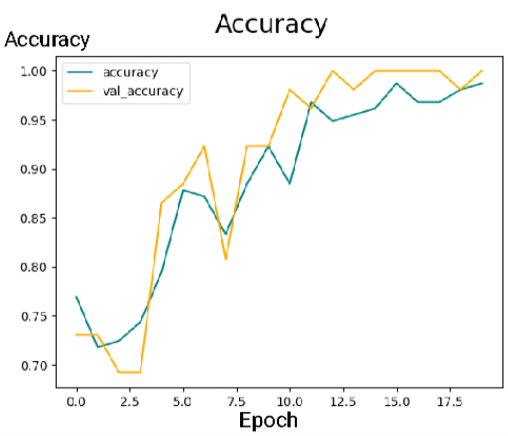

Fig. 6. The accuracy versus epochs graph for scoliosis versus normal classification

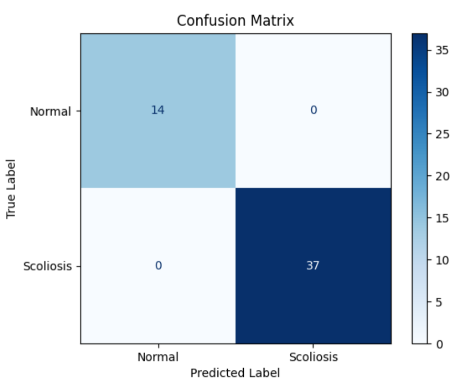

Fig. 7. The confusion matrix for scoliosis versus normal classification

Fig. 7 displays the confusion matrix of the prediction done by the deep learning model. The model was able to correctly predict all normal and scoliosis images according to their class, achieving a test accuracy of 100%.

4.1.2 Spondylolisthesis and Normal Spine

The second task performed by the model is a binary classification of normal spine and spondylolisthesis. Fig. 8 displays examples of images from each class, where image labelled 0 represents the normal spine while 1 represents the spine with spondylolisthesis. The accuracy versus epoch graph is displayed in Fig. 9. The deep learning model was able to achieve training and validation accuracy of more than 90% after three epochs. However, the performance increment rate is small after five epochs.

For the testing dataset, the performance of the deep learning model was able to achieve an accuracy of 100%. This is shown by the confusion matrix in Fig. 10.

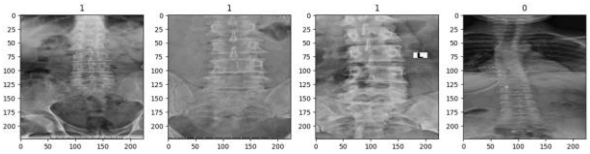

Fig. 8. Labeling of images in spondylolisthesis versus normal classification

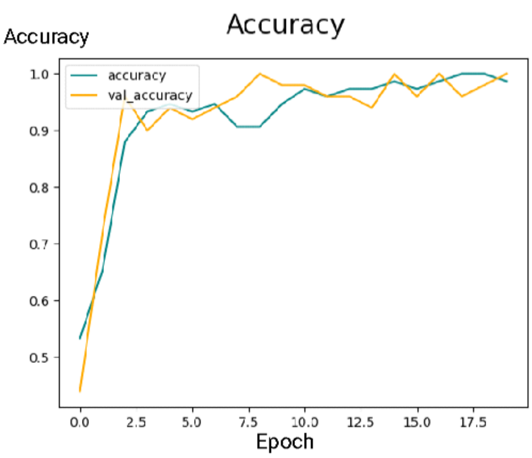

Fig. 9. The accuracy versus epochs graph for spondylolisthesis versus normal classification

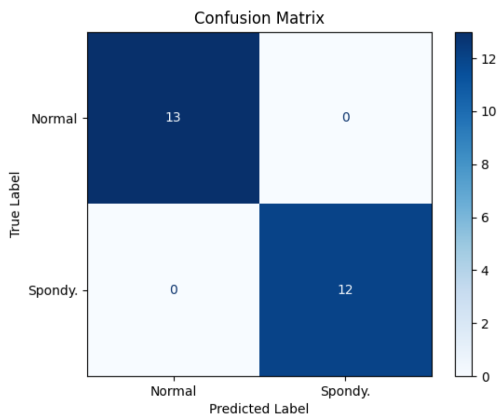

Fig. 10. The confusion matric for spondylolisthesis versus normal classification

4.1.3 Scoliosis, Spondylolisthesis and Normal Spine

The third task applied using the same vertebrae X-ray dataset is multiclass classification which includes all

three classes available in the dataset. The training and validation accuracy of the deep learning model is displayed in Fig. 11. The model was able to correctly predict the class of images in the validation dataset from the epoch cycle of 10 to 17. The training accuracy was able to achieve an accuracy of more than 90% after 7 epochs.
The confusion matrix of the multiclass classification using the test dataset is displayed in Fig. 12. The model was able to correctly classify all the images to their respective classes.

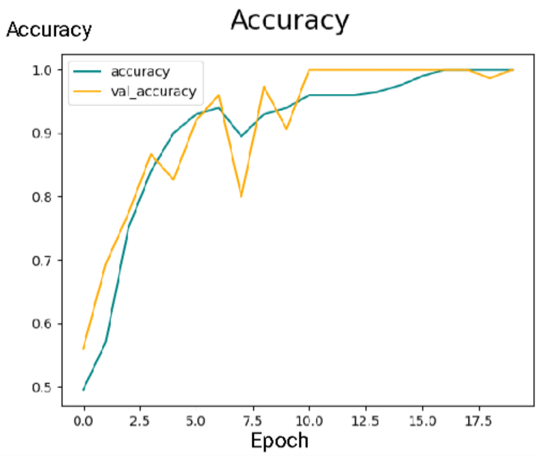

Fig. 11. The accuracy versus epochs for scoliosis, spondylolisthesis, and normal classification

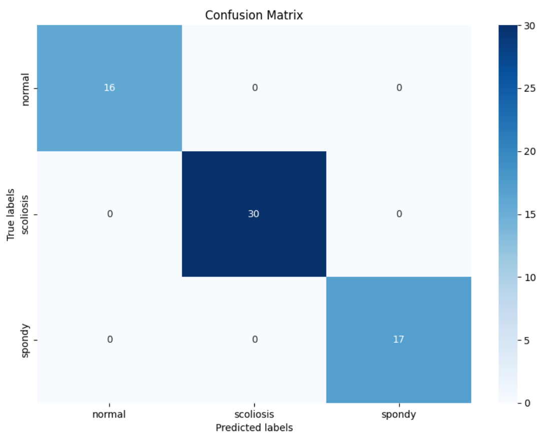

Fig. 12. The confusion matrix for scoliosis, spondylolisthesis, and normal classification

4.2 BUU Spine Dataset

The images used from the BUU Spine Dataset are the lateral images with two classes: lesion and normal spine. Lesion image is labeled as 0 and a normal spine is labeled as 1. This is shown in Fig. 13. The accuracy of the model during the training process is displayed in Fig. 14. The model accuracy increased consistently throughout the training process. The model achieved an accuracy of more than 90% after training the model for 7 epochs.
The confusion matrix visualizing the testing performance of the model for predicting the lesion and normal spine in the BUU spine dataset is displayed in Fig. 15. The model correctly classified most of the images into their respective classes. Out of 80 images in the test datasets, only two images are not correctly classified, where a normal spine is mistakenly classified as a spine with lesion (false positive) and a lesion is mistakenly identified as normal (false negative).

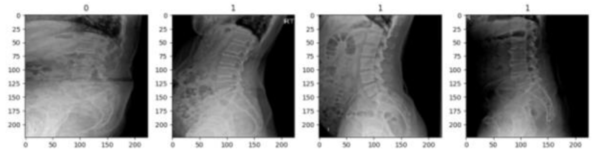

Fig. 13. Labeling of images in lesion versus normal classification

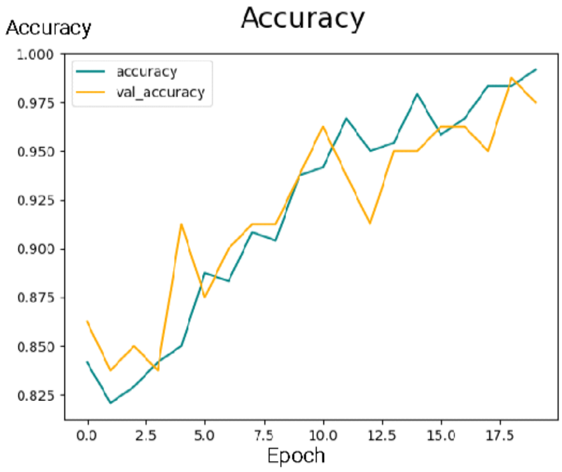

Fig. 14. The accuracy versus epoch graph for lesion version normal classification

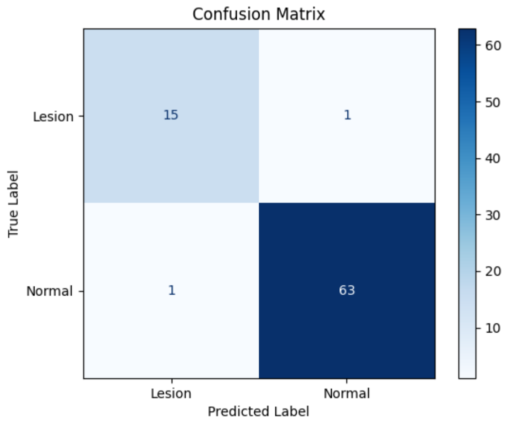

Fig. 15. The confusion matrix for lesion versus normal classification

4.3 Summary of Results

The result of the classification task using the deep learning model is summarized in Table 2. The table displays the training, validation, and testing accuracy of the deep learning model. The training accuracy for all is above 98%. The model obtained a validation and testing accuracy of 100% on all three classification tasks of the vertebrae x-ray dataset. The dataset has a good distribution of images to each of the classes, where there are 71 normal, 188 scoliosis, and 79 spondylolisthesis images respectively.
Lower validation and testing accuracy (97.5%) was achieved on normal versus lesion classification in the BUU Spine Dataset. This could be due to difficulty in distinguishing normal spines from spines with lesions due to an imbalance of data ratio in each class. Out of 400 images in the dataset, only 59 images were spine with lesion. The rest of the images, 341 x-rays are normal spine. Hence, the model is not adequately trained to distinguish the lesion in spine x-ray.

Table 2. Summary of the result classification

Classification Task	Training Accuracy	Validation Accuracy	Testing Accuracy
Normal/Scoliosis	0.9872	1.0	1.0
Normal/Spondy.	0.9867	1.0	1.0
Normal/Spondy. / Scoliosis	1.0	1.0	1.0
Normal/Lesion (Lateral View)	0.9917	0.9750	0.9750

5. CONCLUSION

In this study, a deep learning model was developed for spine x-ray abnormalities classification tasks. The classes included in this study are normal, spondylolisthesis, scoliosis, and lesion. The model achieved a high accuracy of more than 97.5%. Although the accuracy is high, further analysis needs to be done to ensure the algorithm is using the correct features for classification. This can be achieved using visualization algorithms such as Grad-cam [35]. There is a chance that the deep learning model was trained to extract information from irrelevant parts of the image rather than focusing on the spine. If this happens, the model performance will reduce when tested using completely new data due to lower generalizability. Grad-cam provides a heat map that can be used to provide a way to visualize the parts that the model focuses on more to provide the classification.

6. ACKNOWLEDGEMENTS

This research is funded by the Telekom Research & Development (TMR&D) research grant, with grant number: RDTC/231094.

7. REFERENCES

[1] Janai J, Güney F, Behl A, Geiger A. Computer vision for autonomous vehicles. Foundations and Trends in Computer Graphics and Vision 2020;12. https://doi.org/10.1561/0600000079.

[2] Pham LH, Nguyen-Ngoc Tran D, Nguyen HH, Tran THP, Jeon HJ, Jeon HM, et al. DeepACO: A Robust Deep Learning-based Automatic Checkout System. IEEE Computer Society Conference on Computer Vision and Pattern Recognition Workshops, vol. 2022- June, IEEE Computer Society; 2022, p. 3106–13. https://doi.org/10.1109/CVPRW56347.2022.00350.

[3] Taiwo O, Ezugwu AE, Oyelade ON, Almutairi MS. Enhanced Intelligent Smart Home Control and Security System Based on Deep Learning Model. Wirel Commun Mob Comput 2022;2022. https://doi.org/10.1155/2022/9307961.

[4] Ahmad MSZ, Ab. Aziz NA, Ghazali AK. Development of Automated Attendance System Using Pretrained Deep Learning Models. International Journal on Robotics, Automation and Sciences 2024;6:6–12. https://doi.org/10.33093/ijoras.2024.6.1.2.

[5] Darwin B, Dharmaraj P, Prince S, Popescu DE, Hemanth DJ. Recognition of bloom/yield in crop images using deep learning models for smart agriculture: A review. Agronomy 2021;11. https://doi.org/10.3390/agronomy11040646.

[6] Ding Z, Zhou J, Du G, Zhao S, Furukawa T, Lu K. A Two-model Automatic Towel Defect Detection Method Based on YOLOv5. International Exchange and Innovation Conference on Engineering and Sciences, 2022. https://doi.org/10.5109/5909122.

[7] Lo JH, Lin LK, Cheng HP, Hung CC. Deep Learning-based Image Recognition for Disaster Prevention Application. International Exchange and Innovation Conference on Engineering and Sciences, 2022. https://doi.org/10.5109/5909124.

[8] Suganyadevi S, Seethalakshmi V, Balasamy K. A review on deep learning in medical image analysis. Int J Multimed Inf Retr 2022;11. https://doi.org/10.1007/s13735-021-00218-1.

[9] Thanoon MA, Zulkifley MA, Mohd Zainuri MAA, Abdani SR. A Review of Deep Learning Techniques for Lung Cancer Screening and Diagnosis Based on CT Images. Diagnostics 2023;13. https://doi.org/10.3390/diagnostics13162617.

[10] Li M, Jiang Z, Shen W, Liu H. Deep learning in bladder cancer imaging: A review. Front Oncol 2022;12. https://doi.org/10.3389/fonc.2022.930917.

[11] Mahoro E, Akhloufi MA. Applying Deep Learning for Breast Cancer Detection in Radiology. Current Oncology 2022;29:8767–93. https://doi.org/10.3390/curroncol29110690.

[12] Chavda M, Degadwala S. A Comprehensive Review on Deep Learning Approach for Prostate Cancer Gleason Grading. International Journal of Scientific Research in Computer Science, Engineering and Information Technology 2023:270–5. https://doi.org/10.32628/cseit2361046.

[13] Singh N. A Review of Brain Tumor Segmentation and Detection Techniques through MRI. vol. 103. 2014.

[14] Zeng C, Gu L, Liu Z, Zhao S. Review of Deep Learning Approaches for the Segmentation of Multiple Sclerosis Lesions on Brain MRI. Front Neuroinform 2020;14. https://doi.org/10.3389/fninf.2020.610967.

[15] Balwant MK. A Review on Convolutional Neural Networks for Brain Tumor Segmentation: Methods, Datasets, Libraries, and Future Directions. IRBM 2022;43. https://doi.org/10.1016/j.irbm.2022.05.002.

[16] Hafiza Akter Munira, Md. Saiful Islam. Multi-Classification of Brain MRI Tumor Using ConVGXNet, ConResXNet, and ConIncXNet. Proceedings of International Exchange and Innovation Conference on Engineering & Sciences (IEICES) 2022;8. https://doi.org/10.5109/5909087.

[17] Hafiza Akter Munira, Md. Saiful Islam. Multi-Classification of Brain MRI Tumor Using ConVGXNet, ConResXNet, and ConIncXNet. Proceedings of International Exchange and Innovation Conference on Engineering & Sciences (IEICES) 2022;8:169–75. https://doi.org/10.5109/5909087.

[18] Meena T, Roy S. Bone Fracture Detection Using Deep Supervised Learning from Radiological Images: A Paradigm Shift. Diagnostics 2022;12. https://doi.org/10.3390/diagnostics12102420.

[19] Mahendrakar P, Kumar D, Patil U. A Comprehensive Review on MRI-based Knee Joint Segmentation and Analysis Techniques. Current Medical Imaging Formerly Current Medical Imaging Reviews 2023;20.

https://doi.org/10.2174/157340562066623051509055 7.
[20] Tragaris T, Benetos IS, Vlamis J, Pneumaticos S. Machine Learning Applications in Spine Surgery. Cureus 2023. https://doi.org/10.7759/cureus.48078.
[21] Saeed MU, Dikaios N, Dastgir A, Ali G, Hamid M, Hajjej F. An Automated Deep Learning Approach for Spine Segmentation and Vertebrae Recognition Using Computed Tomography Images. Diagnostics 2023;13. https://doi.org/10.3390/diagnostics13162658.
[22] An CH, Lee JS, Jang JS, Choi HC. Part Affinity Fields and CoordConv for Detecting Landmarks of Lumbar Vertebrae and Sacrum in X-ray Images. Sensors 2022;22. https://doi.org/10.3390/s22228628.
[23] Cina A, Bassani T, Panico M, De Luca A, Masharawi Y, Brayda-Bruno M, et al. 2-step deep learning model for landmarks localization in spine radiographs. Sci Rep 2021;11:9482. https://doi.org/10.1038/s41598-021-89102-w.
[24] Tavana P, Akraminia M, Koochari A, Bagherifard A. Classification of spinal curvature types using radiography images: deep learning versus classical methods. Artif Intell Rev 2023;56:1–13291. https://doi.org/10.1007/s10462-023-10480-w.
[25] Yahara Y, Tamura M, Seki S, Kondo Y, Makino H, Watanabe K, et al. A deep convolutional neural network to predict the curve progression of adolescent idiopathic scoliosis: a pilot study. BMC Musculoskelet Disord 2022;23:610. https://doi.org/10.1186/s12891-022-05565-6.
[26] Yi W, Zhao J, Tang W, Yin H, Yu L, Wang Y, et al. Deep learning-based high-accuracy detection for lumbar and cervical degenerative disease on T2-weighted MR images. Eur Spine J 2023;32:3807–14. https://doi.org/10.1007/s00586-023-07641-4.
[27] Zhang J, Liu J, Liang Z, Xia L, Zhang W, Xing Y, et al. Differentiation of acute and chronic vertebral compression fractures using conventional CT based on deep transfer learning features and hand-crafted radiomics features. BMC Musculoskelet Disord 2023;24:165. https://doi.org/10.1186/s12891-023-06281-5.
[28] Sindhura DN, Pai RM, Bhat SN, Manohara Pai MM. Automatic type Identification of Sub - Axial Vertebral Column Fractures using Deep learning Technique. J Phys Conf Ser 2023;2571:12003. https://doi.org/10.1088/1742-6596/2571/1/012003.
[29] Iyer S, Blair A, White C, Dawes L, Moses D, Sowmya A. Vertebral compression fracture detection using imitation learning, patch based convolutional neural networks and majority voting. Inform Med Unlocked 2023;38:101238. https://doi.org/10.1016/j.imu.2023.101238.
[30] Park J, Yang J, Park S, Kim J. Deep Learning-Based Approaches for Classifying Foraminal Stenosis Using Cervical Spine Radiographs. Electronics (Basel) 2022;12:195. https://doi.org/10.3390/electronics12010195.
[31] Dzierżak R, Omiotek Z. Application of Deep Convolutional Neural Networks in the Diagnosis of Osteoporosis. Sensors (Basel) 2022;22:8189. https://doi.org/10.3390/s22218189.
[32] Burapha University. BUU Spine Dataset n.d. https://services.informatics.buu.ac.th/spine/ (accessed May 14, 2024).
[33] Géron A. Hands-on machine learning with Scikit-Learn and TensorFlow : concepts, tools, and techniques to build intelligent systems. 2019.
[34] Kingma DP, Ba JL. Adam: A method for stochastic optimization. 3rd International Conference on Learning Representations, ICLR 2015 - Conference Track Proceedings, 2015.
[35] Selvaraju RR, Cogswell M, Das A, Vedantam R, Parikh D, Batra D. Grad-CAM: Visual Explanations from Deep Networks via Gradient-based Localization 2016. https://doi.org/10.1007/s11263-019-01228-7.